Eng. Sci., 2021, **14**, 59–68

Engineered Science

DOI: https://dx.doi.org/10.30919/es8d1161

A Subcutaneously Injected SERS Nanosensor Enabled Long-term *in Vivo* Glucose Tracking

Yikun Huang,[1] Yi Luo,[2] Haomin Liu,[3] Xiuling Lu,[3] Jing Zhao[2] and Yu Lei[1, 4*]

Abstract

Diabetes is a major health problem around the world. *In vitro* enzyme-based glucose test strips have dominated the self-monitoring of blood glucose; however, the pain associated with fingerstick often deters patients from frequent monitoring. In this study, we report a subcutaneously injected surface enhanced Raman scattering (SERS) nanosensor to enable long-term *in vivo* glucose tracking. The glucose-responsive SERS nanosensor was prepared by self-assembling of a monolayer of 4-mercaptophenylboronic acid (MPBA) on gold nanoparticles (AuNPs). The aggregates of MPBA-functionalized AuNPs (MPBA-AuNPs) resulted in Raman signal enhancement of MPBA, and thus endowed MPBA-AuNPs serving as functional SERS nanosensor for glucose monitoring. After the demonstration of *in vitro* and *ex vivo* glucose detection, the glucose-responsive SERS nanosensor was subcutaneously injected into nude mice to investigate its ability in long-term *in vivo* glucose tracking. The trends obtained from glucose monitoring using a portable Raman probe in mice show a reasonable match with the ones derived from blood using a commercial glucose meter over a period of 60 days. The good biocompatibility of the subcutaneously injected MPBA-AuNPs nanosensor was also validated through histological analysis. All these features indicate that the as-prepared SERS nanosensor holds great potential in long-term glucose tracking.

Keywords: In vivo; Long-term; Glucose detection; SERS; Au nanoparticle; MPBA.
Received: 16 November 2020; Accepted: 09 December 2020.
Article type: Research article.

1. Introduction

Diabetes mellitus is a metabolic disorder in which body is unable to control blood glucose level.[1] This disease has become a significant and expanding public health problem in USA.[2] According to national diabetes statistics report, diabetes was the seventh leading cause of death in the United States in 2015, and 30.3 million people (9.4% of the US population) have diabetes in 2017. Diabetic patients need regular and daily blood monitoring to control the blood glucose level.[3] Currently strip-based electrochemical glucose self-testing systems rely on glucose oxidase (GOD)-based or glucose dehydrogenase (GDH)-based detection methods.[4] Although they dominate the market and are widely used by diabetic patients at home, the pain associated with the fingerstick can deter patients from frequent monitoring,[5] thus resulting in a poor tracking of blood glucose variations in real time.[6,7] As a result, there is an urgent need to develop non-invasive or minimally invasive methods for long-term monitoring of blood glucose.

Enzyme-based amperometric continuous *ex vivo* and *in vivo* monitoring of blood glucose was first proposed in the 1970's and 1980's, respectively.[8,9] *In vivo* continuous glucose monitoring would generate real-time data about the change of blood glucose levels. However, the development of reliable implantable glucose sensors is still very challenging, as undesirable interactions between the implanted device and the biological medium cause rapid deterioration of amperometric sensor performance upon implantation.[10] In addition, due to biofouling of the electrode surface by proteins and coagulation factors and the risk of thromboembolism, most continuous sensors do not measure blood glucose directly, and their

[1] *Department of Biomedical Engineering, University of Connecticut, 260 Glenbrook Road, Storrs, CT 06269, USA.*
[2] *Department of Chemistry, University of Connecticut, 261 Glenbrook Road, Storrs, CT 06269, USA.*
[3] *Department of Pharmaceutical Sciences, University of Connecticut, 69 North Eagleville Road, Storrs, CT 06269, USA.*
[4] *Department of Chemical and Biomolecular Engineering, University of Connecticut, 191 Auditorium Road, Storrs, CT 06269, USA.*
* *Email:* yu.lei@uconn.edu (Y. Lei)

stability and calibration to blood glucose levels have been proven difficult.[11] Recently, a tissue glucose amperometric sensor implanted for more than one year in an animal was reported, with promising results.[12] However, the need for surgical implantation of the device and potential adverse medical effects may limit its use by diabetic patients at home. Despite extensive research efforts in these areas over the past years, no FDA approved reliable method is presently available for continuous long-term implantable tissue glucose monitoring.[10] Alternatively, extensive efforts have been devoted over the past decade toward the design of subcutaneously implantable needle-type electrodes for short-term measurement of glucose concentrations in interstitial fluid, which reflect the blood glucose level.[10,13-15] To date, several needle-type continuous glucose sensors have been approved by U.S. FDA, including the Guardian REAL-time continuous glucose monitoring system, Dexcom SEVEN Plus, Medtronic's MiniMed Paradigm® REAL-Time System, and iPro2. Although these 'under-the-skin' devices can display updated real-time glucose concentrations every one to five minutes, their application is limited because of the inconvenience associated with continuously wearing the device on the upper arm, the short lifetime (3-7 days) due to biofouling problems, as well as poor stability associated with the enzyme used.[16] Continuous subcutaneous glucose monitoring can also be achieved without direct contact between the interstitial fluid and transducer by using the microdialysis technique.[17,18] For example, glucoDay (Menarini, Florence, Italy) and SCGM (Roche, Mannheim, Germany) are based on a microdialysis technique. However, major challenges to long-term subcutaneous continuous glucose monitoring, including biocompatibility, calibration, drift and long-term stability, specificity, linearity, and miniaturization, still hamper their routine clinical usefulness. Other methods such as transdermal glucose sensor were also proposed as an alternative. Approved by the U.S. FDA, the GlucoWatch Biographer (Cygnus, Inc., Redwood City, CA, USA), is a watch-like electrochemical device based on transdermal extraction of interstitial fluid by reverse iontophoresis. However, it has not gained wide acceptance due to long warm up time, false alarms, inaccuracy, skin irritation, and sweating. As a result, the GlucoWatch was withdrawn from the market after 2008. Thus, new continuous *in vivo* glucose-sensing strategies need to be developed. Non-invasive and minimally invasive optical approaches come out as an alternative.[19,20] Optical glucose sensors use physical properties of light in the interstitial fluid or the anterior chamber of the eye. To date, different optical techniques such as polarimetry,[21,22] Raman spectroscopy,[23] infrared absorption spectroscopy,[24] photoacoustics,[25] and optical coherence tomography[26] have been studied for non-invasive glucose detection. However, due to the intrinsic weak optical signal of glucose and the optical interference from tissue, their application is greatly limited.

As one of the most powerful and attractive analytical techniques, surface enhanced Raman scattering (SERS) offers many advantages in analyte sensing, including high sensitivity, good capability of anti-disturbance and easiness of operation.[27-30] Raman spectroscopy directly measures the vibrational modes of molecules, therefore, can be used to identify molecules and quantify their amount. However, the Raman signal is often weak. Raman signal can be highly enhanced when target molecules are in close proximity to a metal surface with nanoscale structures.[31] Due to its ability to provide spectroscopic fingerprint of molecules, and the giant electromagnetic field enhancement enabled by localized surface plasmon resonance (LSPR)[32] of noble metal nanoparticles, SERS allows for accurate analysis of target molecule. This feature enables SERS-based sensing technique to be applied for real world applications.[33-35] SERS enhancement relies on several conditions: one, the target molecule should be in close proximity with the surface; two, the LSPR of the SERS substrates should ideally be matched with the frequency of the excitation laser, and the scattered photons; and three, the SERS substrates should have sharp edges and corners, which would provide high electric field enhancement to increase the SERS signal. Although SERS is a powerful analytical method, its application for *in vivo* glucose detection is limited due to the small Raman scattering cross-section, the low affinity of glucose molecules with metal surfaces, and the poor biocompatibility of SERS sensing materials.[36] Several SERS substrates were engineered to address these challenges. Van Dyne *et al.* reported the first direct detection of glucose via SERS,[37-39] in which a metal substrate with chemical functionalization was designed to increase the affinity of glucose molecule with metal surface. Specifically, the self-assembled monolayer (SAM) deposited on the silver substrate can partition glucose molecules into the SAM reversibly, resulting in detectable Raman spectra of glucose at different concentrations. However, the signal is relatively week, and the device is too complicated for *in vivo* detection. To address the challenge above, SERS-based indirect glucose detection method was also developed. Recently, our group reported a 4-mercaptophenylboronic acid (MPBA) functionalized Ag nanorod arrays for SERS-based glucose monitoring, which shows remarkable sensing ability.[40] However, the potential toxicity of Ag limits the further *in vivo* application of this SERS glucose sensor.

Herein, we report a subcutaneously injected SERS nanosensor to enable noninvasive, long-term *in vivo* glucose monitoring via determination of glucose concentration in the interstitial fluid in dermal layer of skin. Fig. 1 presents the schematic of the subcutaneously injected glucose-responsive SERS

nanosensor for *in vivo* glucose monitoring. In brief, gold nanoparticles (AuNPs) were employed as the SERS substrate because of their high biocompatibility and Raman signal enhancement, while MPBA was chosen as glucose receptor due to its SH- group for covalently anchoring on AuNPs and its reversible binding affinity with glucose through its boronic acid motif. The glucose-responsive SERS nanosensor was prepared by self-assembling of a monolayer of MPBA on AuNPs. After the validation of the concept using *in vitro* and *ex vivo* test, the as-prepared SERS nanosensor was subcutaneously injected in mice for *in vivo* long-term glucose tracking. A commercial glucose meter (HealthPro^{TM} Glucose monitoring system) was simultaneously employed to track the blood glucose variation using the blood withdrawn from the mouse tail vein. *In vivo* SERS detection shows strong signal without any optical interference from skin. Over a period of 60 days, the trends obtained from SERS nanosensor for three mice shows a reasonable match with the ones derived from the commercial glucose meter. The good biocompatibility of the subcutaneously injected MPBA-AuNPs nanosensors was also validated through histological analysis.

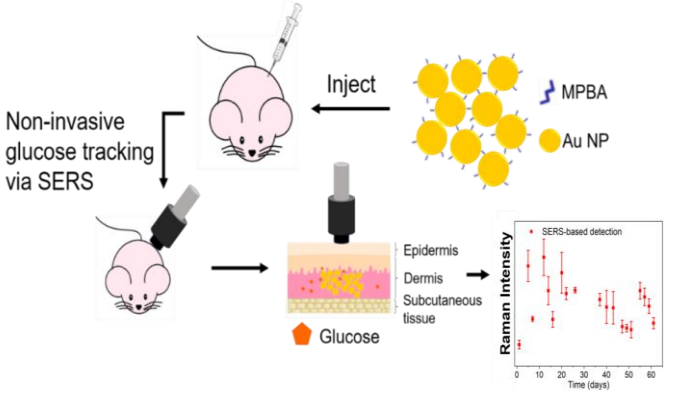

Fig. 1. Schematic of the subcutaneous-injectable glucose-responsive SERS nanosensor for long-term *in vivo* glucose tracking. The glucose-responsive SERS nanosensor was prepared by self-assembling of a monolayer of 4-mercaptophenylboronic acid (MPBA) on gold nanoparticles (AuNPs).

2. Experimental

2.1 Chemicals and materials

All chemicals used were analytical grade and used as received without further purification. Gold (III) chloride trihydrate (≥99.9% trace metals basis), hydroxylamine hydrochloride, glucose, 4-mercaptophenylboronic acid (MPBA) and ethanol were purchased from Sigma-Aldrich. Sodium citrate and phosphate buffered saline (10× solution) were purchased from Fisher Scientific. All aqueous solution was prepared by ultrapure water (Milli-Q, Millipore, 18.2 MΩ·cm resistivity).

2.2 Au nanoparticles synthesis and MPBA-functionalization of Au nanoparticles

A seed mediated method was used to synthesize 120 nm AuNPs according to a previous report.[41] To prepare MPBA-functionalized AuNPs, 200 mL of 120 nm citrate stabilized Au nanoparticles was centrifuged at 1000 rpm for 30 min at 4 °C to concentrate the AuNPs. Then, the resulting AuNPs pellet was treated with 10 mL of 1 mM MPBA ethanolic solution with gentle mixing. After 12 hr reaction between MPBA and Au nanoparticles at room temperature under shaking, the excessive MPBA molecule was removed by centrifugation at 800 rpm for 2 min followed by ethanol washing. This process was repeated 5 times to ensure the complete removal of unbounded MPBA. The MPBA-AuNPs pellet was dried in vacuum for further applications.

3. Characterization

3.1 Transmission Electron Microscopy (TEM) and Scanning Electron Microscopy (SEM) Imaging

120 nm Au nanoparticle suspension was drop casted on a carbon-coated TEM grid (Electron Microscopy Sciences) and allowed to dry in air for TEM imaging. FEI Tecnai G2 Spirit BioTWIN was then used to acquire the TEM images under the acceleration voltage of 80 kV. To prepare the SEM sample, 10 µL of the 120 nm Au nanoparticles solution was drop-cast onto a glass slide and dried in air. The glass slide was then coated with a gold thin film using a sputter coater to increase the conductivity of the SEM sample. FEI Nova NanoSEM 450 was then used to acquire the SEM images.

3.2 SERS measurement

A portable Raman spectrometer (QE Pro, Ocean Optics) with an InPhotonics fiber optic Raman probe was used to collect the Raman spectra. A 785 nm laser (operated at 38 mW) was used to excite the samples. For each Raman measurement, the spectrum was integrated for 5 s. A homemade black box was used during the SERS measurement for characterization, *in vitro*, and *ex vivo* experiments in order to eliminate the potential interference from environmental light. To prove the successful functionalization of MPBA on AuNPs, 5 µL of MPBA-AuNPs suspension was dropped on a clean silicon wafer and dried for SERS measurement. For *in vivo* experiment, a 3D printed black-color plastic probe holder was fixed on the laser probe to ensure the distance of 7 mm between animal skin and the detector. Such holder also mitigated the interference from environmental light to certain degree.

3.3 *In vitro* and *ex vivo* glucose detection using MPBA-AuNPs based SERS nanosensors

For *in vitro* glucose detection, 5 µL of MPBA-AuNPs suspension was first centrifuged in 1.5 mL microcentrifuge tube and the supernatant was decanted. The MPBA-AuNPs formed a thin film on the wall at the bottom of the tube. The tube was then cut with a razor blade to remove the top part and the bottom part of 7 mm tall with the thin film on the wall was kept for subsequent SERS measurements. Next, 10 µL of PBS buffer solution was dropped onto the as-prepared MPBA-AuNPs thin-film coated tube. After a reaction time of 10 min, SERS spectra were measured three times, and the average

value was used for data analysis. For each subsequent experiment, 5 μL solution was withdrawn from the as-prepared MPBA-AuNPs thin-film coated tube first and then 5 μL glucose solution with an appropriate concentration was loaded to vary glucose concentration in the well while maintain the same total working volume (10 μL) for each detection. The final concentration in the well is the average concentration of the old solution in the well and the new solution added.

For *ex vivo* glucose detection, fresh chicken skin collected from chicken wing (purchased from a local grocery store) was used. A syringe needle was used to penetrate the chicken skin and deliver the MPBA-AuNPs to the dermis layer. The chicken skin with subcutaneously injected SERS nanosensor was then stored in pH 7.4 PBS buffer. For *ex vivo* detection, glucose concentration in PBS buffer was varied through adding appropriate amount of glucose powder to maintain the same total working volume of PBS buffer solution but with gradually increased glucose concentrations. After glucose powder dissolved in PBS buffer, the chicken skin with injected SERS nanosensor was immersed in the glucose solution for 30 min to allow sufficient diffusion of glucose to reach equilibrium, and Raman spectra were then collected using the portable Raman system.

3.4 *In vivo* glucose detection using MPBA-AuNPs based SERS nanosensors

In vivo experiments were conducted using athymic nude mice. All *in vivo* experiments followed the protocol approved by Institutional Animal Care and Use Committee (IACUC) at the University of Connecticut. Humane use and care of vertebrate animals were guaranteed in the research. To subcutaneously inject SERS nanosensor into mouse, the dried MPBA-AuNPs aggregates were re-suspended in 50 μL pH 7.4 PBS buffer and sonicated for 5 min to form a uniform suspension. 50 μL of MPBA-AuNPs suspension was then loaded into a sterile Hamilton syringe and subcutaneously injected into the mouse. A micro-computed tomography (The IVIS® SpectrumCT, PerkinElmer) was employed to track the injected MPBA-AuNPs nanosensors in mice. A series of CT images were taken before and after injection. Animals were kept under isoflurane anesthesia (2%, O_2 0.5 liter/min) during injection and imaging sessions to avoid the movement of the mouse. After the injection wound was healed, the glucose detection by non-invasive SERS monitoring was collected, spanning 60 days. For each detection, 10 SERS spectra were collected by moving the probe randomly on the injection site of sensing material due to the small laser spot of portable Raman probe. For the data analysis of SERS-based detection, the two maximum and two minimum values were removed and the average value of remaining six intensities was used for each time point. Meanwhile, a commercial glucose meter (HealthPro™ Glucose monitoring system) was used to measure the glucose concentration of blood withdrawn from the mouse tail vein.

4. Results and discussion

4.1 Characterization of MPBA-AuNPs

SEM and TEM were used to study the morphology of the Au nanoparticle before and after MPBA functionalization. As shown in Fig. 2a (inset), the average diameter of the Au nanoparticle is ~120 nm. Before MPBA functionalization, the as-prepared AuNPs were well dispersed on the substrate without obvious aggregation. After treatment of AuNPs with MPBA, MPBA was covalently anchored on AuNPs via Au-S bond. The original citrate ligands on AuNPs would not affect this process and was replaced by MPBA molecules due to the high binding ability between thiol and Au.[42, 43] After ligand exchange, hydroxyl group of MPBA molecules anchored on different AuNPs would form hydrogen bond, which can cross-link the MPBA-AuNPs to from aggregates, in good agreement with the experimental observation. The localized surface plasmon resonance of AuNPs and MPBA-AuNPs aggregates were investigated via UV-vis absorption spectrometry. As shown in Fig. S1, there is no sharp peak observed in the spectrum of MPBA-AuNPs, indicating the formation of aggregates after modification with MPBA. This result was further supported by the SEM and TEM images in Fig. 2. The aggregates exhibit highly compact structure with small gaps among the AuNPs (Inset of Fig.2b), resulting in numerous hot spots for enhanced SERS signal.[44-46]

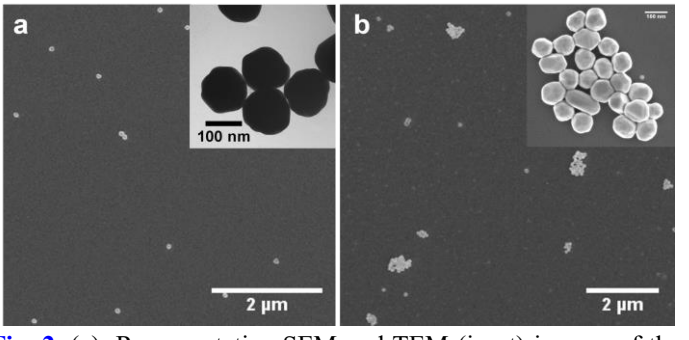

Fig. 2. (a). Representative SEM and TEM (inset) images of the as-prepared 120 nm Au nanoparticles; (b). A typical SEM image of MPBA-AuNPs aggregates with an enlarged image (inset).

Furthermore, AuNPs before and after MPBA functionalization were examined using Raman spectroscopy. The corresponding Raman spectra are shown in Fig. 3a. Herein, 785 nm laser was used for excitation and further applications because it is the most commonly used near-infrared wavelength which would benefit *in vivo* experiment.[47,48] Compared with the Raman spectrum of AuNPs, MPBA-functionalized AuNPs exhibit intense characteristic Raman peaks of MPBA, confirming that MPBA was successfully decorated on the surface of the AuNPs. More specifically, the two strong peaks at 1073 cm^{-1} and 1586 cm^{-1}, correspond to the CS stretching (1073 cm^{-1}) and CC stretching (1586 cm^{-1}) modes of MPBA.[49] These two peaks can be considered as the Raman fingerprint for *in vivo* glucose detection since the skin tissue does not generate significant signal at these two wavelengths (c.f. Inset in Fig.6c). In

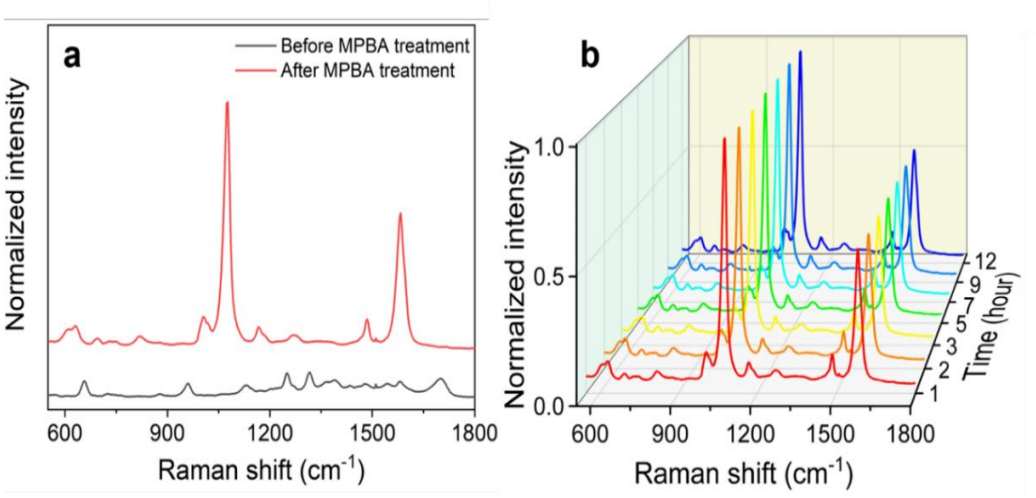

Fig. 3. (a). Raman spectra of Au nanoparticles before and after MPBA functionalization; (b). Raman spectra of the deposited MPBA-AuNPs collected over 12h, indicating good stability of the SERS nanosensor.

addition, the Raman signal of MPBA-AuNPs tracking (Fig. 3b) indicates that the SERS nanosensor possesses good stability without signal loss over 12h, allowing for long-term glucose monitoring. These results demonstrate that MPBA-functionalized AuNPs hold a great promise for *in vivo* glucose monitoring.

4.2 *In vitro* and *ex vivo* glucose detection

Although pristine AuNPs cannot detect glucose through SERS directly (data not shown), MPBA-functionalized AuNPs show glucose concentration dependent behavior, thus offering an excellent method for indirect glucose detection. *In vitro* and *ex vivo* glucose detection was first carried out before *in vivo* application. Fig. 4b shows the collected SERS spectra of the MPBA-AuNPs substrate at different glucose concentrations (covering clinically relevant range) in PBS buffer. It is clear that the MPBA-AuNPs responded to glucose with a concentration-dependent behavior and thus it can serve as glucose-responsive SERS nanosensor. The SERS response of MPBA-functionalized noble metals nanoparticles to glucose could be attributed to orientation and charge transfer related mechanisms.[40] Briefly, MPBA bound to Au surface through thiol-Au interaction. After glucose molecules bound with the boronic acid motif in MPBA, the distance between the phenyl group in MPBA and Au surface becomes shorter because of the orientation change. The phenyl group then experiences a stronger electric-field enhancement from the Au surface. Correspondingly, the SERS signal intensity of MPBA increases with the increase of glucose concentration.[40] In addition, charge transfer mechanism can be another major contributor to the observed enhancement of SERS signal in glucose detection. It was reported that the molecular interaction between glucose and phenylboronic acid can accelerate the electron excitation phenomenon on Au surface.[50] Also, charge transfer effect can be the origin of the significant Raman intensity change of functional groups on benzene ring.[51,52] In this regard, the change of SERS signal intensity could be caused by the reaction of glucose and MPBA molecules, which does not only lead to the electronic state change of benzene ring, but also breaks the symmetry of MPBA anchored on AuNPs.

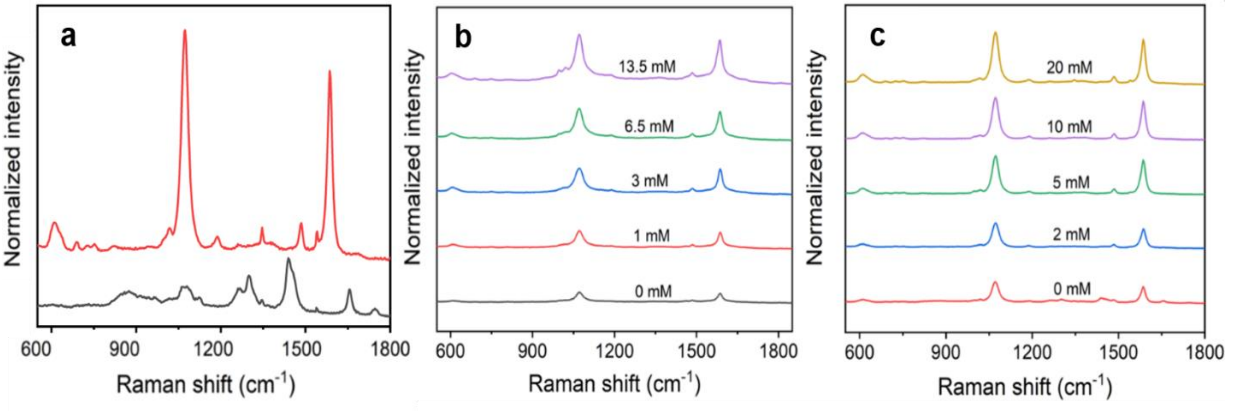

Fig. 4. (a). Raman spectra of chicken skin before (black line) and after (red line) injection of MPBA-AuNPs; (b). Raman spectra of MPBA-AuNPs loaded with PBS buffer solution containing glucose in its clinically relevant concentration ranges; (c). Raman spectra of *ex vivo* glucose detection using chicken skin injected with MPBA-AuNPs.

Furthermore, the SERS nanosensor was evaluated by an *ex vivo* skin model to investigate its feasibility for *in vivo* applications. The Raman spectrum of chicken skin was collected before and after the injection of MPBA-AuNPs. As shown in Fig. 4a, there was no overlap of Raman peaks between MPBA and chicken skin. After the injection of MPBA-AuNPs into chicken skin, a black dot was observed in the skin (Fig. S2), demonstrating that the SERS nanosensor has been successfully delivered into the skin model. Moreover, as shown in Fig. 4c, the strong peaks at 1073 cm^{-1} and 1586 cm^{-1} (originated from MPBA on AuNPs) still existed and responded to glucose with a concentration-dependent behavior. These *in vitro* and *ex vitro* studies paved the road for the following *in vivo* experiment.

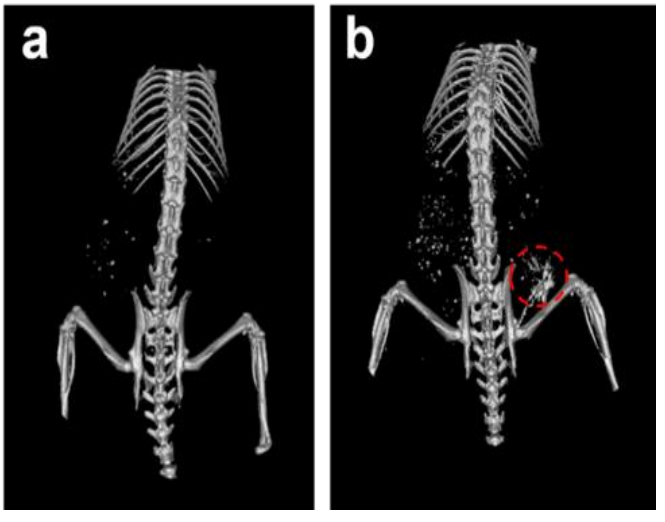

Fig. 5. Micro-CT images of mouse before (a) and after (b) subcutaneous injection of MPBA-AuNPs, indicating the present of SERS nanosensor (red circle indicating the injection site).

4.3 *In vivo* glucose detection

Encouraged by the results from *in vitro* and *ex vivo* glucose sensing experiments, we subcutaneously injected the MPBA-functionalized AuNPs into dermis of mouse skin and performed *in vivo* glucose detection. Dermal layer, an interface between epidermal layer of skin and rest of body, is an ideal location for biocompatible biosensor implantation due to the transmission of interstitial fluid (ISF) in this layer. Although other body fluids like saliva and tear are also widely used for biomarker detection,[53, 54] they cannot be applied for glucose measurement since the glucose level in these fluids shows weak correlation with blood glucose level. Differently, Thennadil and co-works reported that the variation of blood glucose levels can be reflected by the glucose concentration in ISF because there is no long lag time between ISF's and plasma glucose levels when blood glucose concentration changes within a short time.[55] Furthermore, the components in ISF are much simpler than in blood, thus significantly reducing the interference from the co-existing molecules. In addition, the translucent epidermal layer can allow the light transmission and reduce signal loss during the non-invasive SERS detection.

After the injection of SERS nanosensor, a micro-CT was employed to track the injected MPBA-AuNPs in a live mouse. Gold nanoparticles can serve as CT contrast agents for *in vivo* imaging.[56] The high atomic number (Au, 79) and absorption coefficient (5.16 at 100 keV) of gold makes it an ideal contrast agent. Also, interference from bone absorption and soft tissue absorption can be reduce by imaging gold at 80-100 keV.[57] The CT images before injection of MPBA-AuNPs and 3-day post injection (injected sample solution was fully absorbed and injection wound was recovered) are shown in Fig. 5. A large bright area in the right flank of CT images after injection of nanosensor was observed, indicating the presence and successful implantation of MPBA-AuNPs in the mouse. As shown in Fig. 6d after 60-day implantation, there was a long thin intradermal and cutaneous muscle layer full of MPBA-AuNPs aggregates that appeared to be between and possibly within some dermal cells. The particle aggregate was surrounded by a thin layer of proliferating fibroblasts forming a thin capsule around the sensing material. There was no other tissue reaction to the foreign material present. This result also indicates the durability of sensing material and its presence after 60 days of test. Additionally, Raman spectra of mouse skin were collected by the portable Raman system before and after injection of SERS nanosensor. As shown in the inset of Fig. 6c, there is no obvious Raman peak from the mouse skin before injection of MPBA-AuNPs, which would be an advantage for *in vivo* glucose monitoring. A few sharp peaks observed in the Raman spectrum of skin are attributed to the noise from our portable Raman. After injection of MPBA-AuNPs, two new and strong peaks at 1073 cm^{-1} and 1586 cm^{-1} appeared in the Raman spectrum of skin. The peak positions are in good agreement with the peaks observed in *in vitro* and *ex vivo* tests. After tissue surrounding the injection site absorbed the PBS within 24 hours, non-invasive SERS detection was performed to monitor the Raman peak intensity change of MPBA at 1073 cm^{-1}, which can be correlated to the blood glucose concentration. The trend of peak intensity change was plotted and then compared with the trend of blood glucose concentration measured in the blood withdrawn from mouse tail vein using a commercial glucose meter (HealthPro™ Glucose Monitoring System). Due to the wound and the time required for wound healing after blood withdrawing from mouse tail vein, we can only perform very limit times of *in vitro* blood glucose test using mouse tail vein blood every week. We conducted the SERS peak intensity tracking and blood glucose concentration detection for 60 days. Fig. 6a and b show the time course of glucose level and MPBA peak (1073 cm^{-1}) intensity as measured by glucose meter and portable Raman spectrometer, respectively. As we mentioned in experiment part, to reduce the variation causes by small laser spot, ten spectra were collected at each time point. After removal of two maximum and two minimum values, the average of six intensity values is used to represent the SERS result for each detection. Fig 6 shows a representative tracking

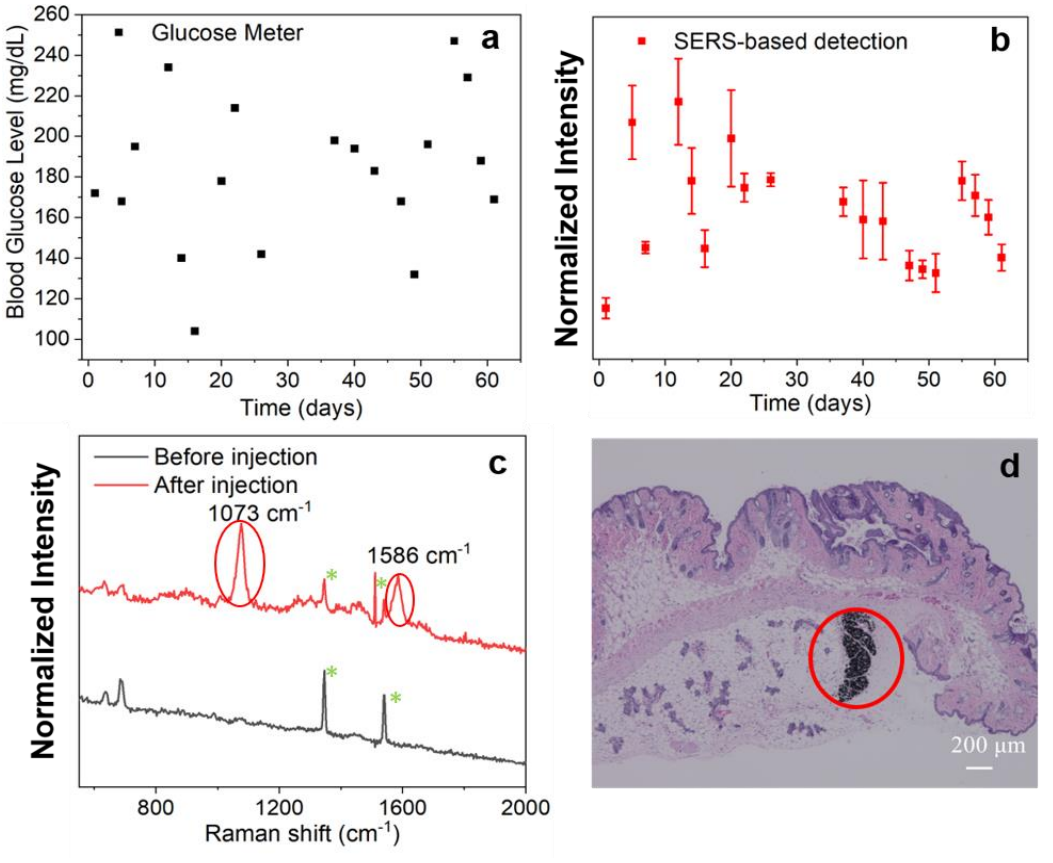

Fig. 6. (a). The trend of glucose concentration changes over 60 days, obtained using blood withdrawn from mouse tail vein and commercial glucose meter (HealthPro™ Glucose Monitoring System); (b). The trend of glucose concentration change over 60 days, obtained using subcutaneously injected MPBA-AuNPs and non-invasive SERS monitoring; (c). Raman spectra of mouse skin before and after sensing material injection. The red circles indicate the MPBA peaks. (Other sharp peaks before and after injection are attributed to the environmental or instrumental noise whose positions are labeled with green stars); (d). Histological analysis result of mouse skin tissue after subcutaneous injection of MPBA-AuNPs. The black dot strip in red circle indicated the position of injected MPBA-AuNPs nanosensor.

results of one mouse, more results from other two mice are presented in Fig. S3. As shown in Fig. 6 and Fig. S3, the plots from SERS sensor show a reasonable match with the ones from blood over a course of 60 days. However, the difference in trends should be further minimized before clinical practice. Several factors could attribute to the difference. First, small laser spot of portable Raman is a main factor that affects the detection accuracy using portable Raman. Although multiple SERS detection was performed to calculate the average, variation cannot be totally overcome in the SERS-based detection considering the uneven distribution of SERS nanosensors after subcutaneous injection. A Raman with the capability to collect the signal over a large area (e.g. all injected SERS nanosensors) could potentially address this issue. Second, the distribution of SERS sensing material may vary between in the early phase and in the latter phase due to endocytosis of MPBA-AuNPs by macrophages which has been confirmed by histology analysis, thus affecting the non-invasive SERS detection accuracy. The matching degree in trends from the plots from SERS and blood glucose meter was improved with the implantation time of SERS nanosensor, which is presumably attributed to stabilization of the implanted SERS nanosensor in skin. To address this challenge, a machine learning algorithm could be employed to decouple the responses from various factors and thus improve the accuracy in the data interpretation. Third, the detection of tail vein blood using commercial glucose meter relied on one-time result due to the limit mouse blood from tail vein and the time for tail wound healing after blood withdrawing. To conduct multiple tests of tail vein blood using commercial glucose meter could also improve the reliability as only 61% of detection results are in 5% variation when the blood glucose concentration is over 75 mg/dL according to the user manual. Although the trend of SERS-based detection cannot perfectly match with that of commercial glucose meter, the results still demonstrate that the subcutaneously injected SERS nanosensor exhibits great potential for long-term and non-invasive blood glucose variation tracking. Moreover, the 60-day test window in this study already surpasses FDA proved needle-type continuous glucose monitoring devices as the wearing period of these sensors are approved up to one week.[58, 59]

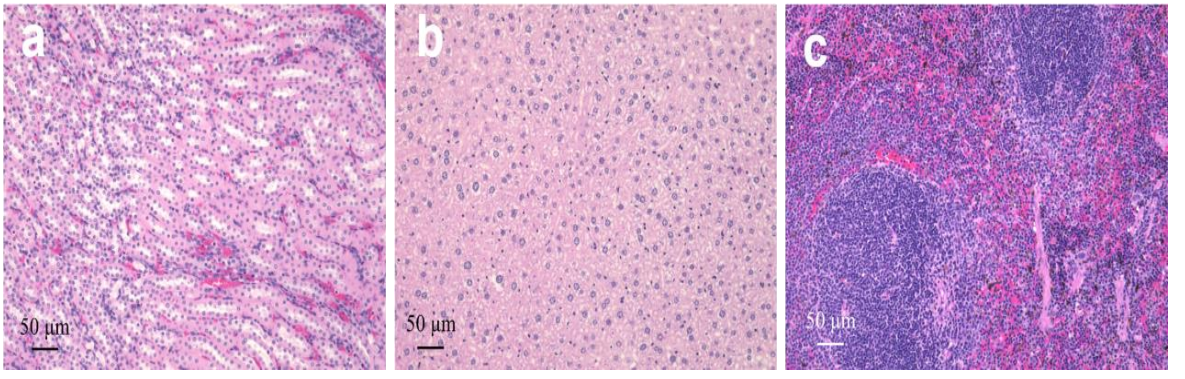

Fig. 7. Histological staining of major organs from the mouse after 60 days of subcutaneously injection of MPBA-AuNPs: Representative H&E-stained slices for (a) kidney, (b) liver, and (c) spleen, respectively.

After *in vivo* study, the biocompatibility of the injected SERS nanosensor was evaluated using histological analysis. The tissue samples from the major organs were collected from the experimental animal for histological analysis. The results are shown in Fig. 7, indicating that no inflammatory response or lesions was found in the major organs. The long-term biocompatibility of the SERS sensing material is validated by histology analysis. The results from *in vivo* experiment and biocompatibility study of our glucose sensor show that it has great potential in the care of diabetes.

5. Conclusions

In summary, we designed a minimal invasive system for long-term monitoring of glucose level via SERS. MPBA was chosen as the probe molecule for glucose detection, while the glucose-responsive SERS nanosensor was prepared by functionalizing AuNPs with MPBA. SEM, TEM, and Raman spectroscopy were employed to characterize the AuNPs and MPBA-AuNPs and validate the successful anchoring of MPBA on the surface of AuNPs. *In vitro* and *ex vivo* glucose detection in clinically relevant glucose concentration ranges was demonstrated using the as-prepared SERS nanosensor. Upon glucose binding with MPBA, the SERS signal of MPBA on AuNPs was significantly enhanced and showed glucose concentration-dependent behavior. Finally, MPBA-AuNPs were subcutaneously injected into nude mice for continuous glucose monitoring. The trends obtained from three mice using a portable Raman probe show a reasonable match with the ones derived from blood withdrawn from mouse tail vein using a commercial glucose meter over a period of 60 days, while the origin of difference was also discussed with several potential solutions. The good biocompatibility of the subcutaneously injected MPBA-AuNPs nanosensor was also validated through histological analysis. All these features indicate that the SERS nanosensor developed in this study holds great potential in long-term glucose monitoring.

Acknowledgment

Y.L, J.Z and X.L.L thank the financial support from US National Science Foundation (EPMD 1509216). The TEM and SEM were performed in part at the Biosciences Electron Microscopy Facility of the University of Connecticut. The histological analysis was performed by Connecticut Veterinary Medical Diagnostic Laboratory. We also would like to thank Xingyu Wang for helpful discussion on data processing. Y.K.H was also partially supported by a fellowship grant from GE's Industrial Solutions Business Unit under a GE-UConn partnership agreement. The views and conclusions contained in this document are those of the authors and should not be interpreted as necessarily representing the official policies, either expressed or implied, of Industrial Solutions or UConn.

Supporting information

Applicable

Conflict of interest

There are no conflicts to declare.

References

[1] A. D. Association, *Diabetes care*, 2010, **33**, S62, doi: 10.2337/dc10-S062.

[2] K. S. Polonsky, *New Engl. J. Med.*, 2012, **367**, 1332-1340, doi: 10.1056/NEJMra1110560.

[3] J. S. Skyler, *J. Med. Chem.*, 2004, **47**, 4113-4117, doi: 10.1021/jm0306273.

[4] S. Park, H. Boo and T. D. Chung, *Anal. Chim. Acta*, 2006, **556**, 46-57, doi: 10.12691/jit-2-1-5.

[5] A. Heller, *Annu. Rev. Biomed. Eng.*, 1999, **1**, 153-175, doi: 10.1146/annurev.bioeng.1.1.153.

[6] Y. Cheng, P. Xiong, C. S. Yun, G. Strouse, J. Zheng, R. Yang and Z. Wang, *Nano Lett.*, 2008, **8**, 4179-4184, doi: 10.1021/nl801696b.

[7] M. A. Arnold and G. W. Small, *Anal. Chem.*, 2005, **77**, 5429-5439, doi: 10.1021/ac050429e.

[8] M. Shichiri, R. Kawamori, Y. Yamasaki, N. Hakui and H. Abe, *Lancet*, 1982, **2**, 1129-1131, doi: 10.1016/s0140-6736(82)92788-x.

[9] A. M. Albisser, B. S. Leibel, T. G. Ewart, Z. Davidovac, C. K. Botz, W. Zingg, H. Schipper and R. Grander, *Dabetes*, 1974, **23**, 397-404, doi: 10.2337/diab.23.5.397.

[10] J. Wang, *Chem. Rev.*, 2008, **108**, 814-825, doi: 10.1021/cr068123a.

[11] J. D. Newman and A. P. F. Turner, *Biosens. Bioelectron.*, 2005, **20**, 2435-2453, doi:10.1016/j.bios.2004.11.012.

[12] D. A. Gough, L. S. Kumosa, T. L. Routh, J. T. Lin and J. Y. Lucisano, *Sci. Transl. Med.*, 2010, **2**, doi: 10.1126/scitranslmed.3001148.

[13] C. Henry, *Anal. Chem.*, 1998, **70**, 594a-598a, doi: 10.1021/ac981937+.

[14] E. Csoregi, D. W. Schmidtke and A. Heller, *Anal. Chem.*, 1995, **67**, 1240-1244, doi: 10.1021/ac00103a015.

[15] D. W. Schmidtke, A. C. Freeland, A. Heller and R. T. Bonnecaze, *P. Natl. Acad. Sci. USA*, 1998, **95**, 294-299, doi: 10.1073/pnas.95.1.294.

[16] M. Cox, *J. Pediatr. Health Car.*, 2009, **23**, 344-347, doi: 10.1097/01.npr.0000430282.47467.5a.

[17] Y. Hashiguchi, T. Uemura, M. Sakakida, K. Kajiwara, K. Nishida and M. Shichiri, *Diabetes Care*, 1994, **17**, 387-396, doi: 10.2337/diacare.17.5.387.

[18] A. Poscia, M. Mascini, D. Moscone, M. Luzzana, G. Caramenti, P. Cremonesi, F. Valgimigli, C. Bongiovanni and M. Varalli, *Biosens. Bioelectron.*, 2003, **18**, 891-898, doi: 10.1016/s0956-5663(02)00216-6.

[19] D. C. Klonoff, *Diabetes Care*, 1997, **20**, 433-437, doi: 10.2337/diacare.20.3.433.

[20] N. S. Oliver, C. Toumazou, A. E. G. Cass and D. G. Johnston, *Diabetic Med.*, 2009, **26**, 197-210, doi: 10.1111/j.1464-5491.2008.02642.x.

[21] W. K. R. Barnikol and N. Weiler, *Biomed. Tech.*, 1995, **40**, 114-120, doi: 10.1515/bmte.1995.40.5.114.

[22] T. W. King, G. L. Cote, R. Mcnichols and M. J. Goetz, *Opt. Eng.*, 1994, **33**, 2746-2753, doi: 10.1117/12.173556.

[23] M. J. Goetz, G. L. Cote, R. Erckens, W. March and M. Motamedi, *IEEE T. Bio-Med. Eng.*, 1995, **42**, 728-731, doi: 10.1109/10.391172.

[24] I. Gabriely, R. Wozniak, M. Mevorach, J. Kaplan, Y. Aharon and H. Shamoon, *Diabetes*, 1999, **48**, A99-A99, doi: 10.2337/diacare.22.12.2026.

[25] H. A. MacKenzie, H. S. Ashton, S. Spiers, Y. C. Shen, S. S. Freeborn, J. Hannigan, J. Lindberg and P. Rae, *Clin. Chem.*, 1999, **45**, 1587-1595, doi:10.1093/clinchem/45.9.1587.

[26] K. V. Larin, M. S. Eledrisi, M. Motamedi and R. O. Esenaliev, *Diabetes Care*, 2002, **25**, 2263-2267, doi: 10.2337/diacare.25.12.2263.

[27] P. Li, R. Dong, Y. Wu, H. Liu, L. Kong and L. Yang, *Talanta*, 2014, **127**, 269-275, doi: 10.1016/j.talanta.2014.03.075.

[28] L. Polavarapu, A. La Porta, S. M. Novikov, M. Coronado-Puchau and L. M. Liz-Marzan, *Small*, 2014, 10, 3065-3071, doi: 10.1002/smll.201400438.

[29] S. Kumar, P. Goel and J. P. Singh, *Sensor Actuat. B-Chem.*, 2017, **241**, 577-583, doi: 10.1016/j.snb.2016.10.106.

[30] H. Dai, Y. Sun, P. Ni, W. Lu, S. Jiang, Y. Wang, Z. Li and Z. Li, *Sensor Actua. B-Chem.*, 2017, **242**, 260-268, doi; 10.1016/j.snb.2016.10.085.

[31] D. L. Jeanmaire and R. P. Van Duyne, *J. Electroanal. Chem. Interf. Electrochem.*, 1977, **84**, 1-20, doi: 10.1016/S0022-0728(77)80224-6.

[32] Z. Yang, A. S. Malinick, T. Yang, W. Cheng and Q. Cheng, *Sensor Actuat. Rep.*, 2020, **2**, 100023, doi; 10.1016/j.snr.2020.100023.

[33] R. G. Freeman, K. C. Grabar, K. J. Allison, R. M. Bright, J. A. Davis, A. P. Guthrie, M. B. Hommer, M. A. Jackson, P. C. Smith, D. G. Walter and M. J. Natan, *Science*, 1995, **267**, 1629-1632, doi: 10.1126/science.267.5204.1629.

[34] M. Fleischmann, P. J. Hendra and A. J. Mcquillan, *Chem. Phys. Lett.*, 1974, **26**, 163-166, doi: 10.1016/0009-2614(74)85388-1.

[35] X. M. Qian and S. M. Nie, *Chem. Soc. Rev.*, 2008, **37**, 912-920, doi: 10.1039/B708839F.

[36] D. A. Stuart, J. M. Yuen, N. Shah, O. Lyandres, C. R. Yonzon, M. R. Glucksberg, J. T. Walsh and R. P. Van Duyne, *Anal. Chem.*, 2006, **78**, 7211-7215, doi: 10.1021/ac061238u.

[37] K. E. Shafer-Peltier, C. L. Haynes, M. R. Glucksberg and R. P. Van Duyne, *J. Amer. Chem. Soc.*, 2003, **125**, 588-593, doi: 10.1021/ja028255v.

[38] O. Lyandres, J. M. Yuen, N. C. Shah, R. P. VanDuyne, J. T. Walsh Jr and M. R. Glucksberg, *Diabetes technol. The.*, 2008, **10**, 257-265, doi: 10.1089/dia.2007.0288.

[39] K. Ma, J. M. Yuen, N. C. Shah, J. T. Walsh Jr, M. R. Glucksberg and R. P. Van Duyne, *Anal. Chem.*, 2011, **83**, 9146-9152, doi: 10.1021/ac202343e.

[40] X. Sun, S. Stagon, H. Huang, J. Chen and Y. Lei, *RSC Adv.*, 2014, **4**, 23382-23388, doi: 10.1039/C4RA02423K.

[41] X. D. Tian, B. J. Liu, J. F. Li, Z. L. Yang, B. Ren and Z. Q. Tian, *J. Raman Spectrosc.*, 2013, **44**, 994-998, doi: 10.1002/jrs.4317.

[42] J. C. Love, L. A. Estroff, J. K. Kriebel, R. G. Nuzzo and G. M. Whitesides, *Chem. Rev.*, 2005, **105**, 1103-1170, doi: 10.1021/cr0300789.

[43] Y. Luo, L. Dube, Y. Zhou, S. Zou and J. Zhao, *Progr. Nat. Sci. Mater. Int.*, 2016, **26**, 449-454, doi: 10.1016/j.pnsc.2016.08.008.

[44] S. Nie and S. R. Emory, *Science*, 1997, **275**, 1102-1106, doi: 10.1126/science.275.5303.1102.

[45] B. Pignataro, A. De Bonis, G. Compagnini, P. Sassi and R.

S. Cataliotti, *J. Chem. Phys.*, 2000, **113**, 5947-5953, doi: 10.1063/1.1316015.
[46] I. W. Sztainbuch, *J. Chem. Phys.*, 2006, **125**, 124707, doi: 10.1063/1.2338029.
[47] J. Mo, W. Zheng, J. J. Low, J. Ng, A. Ilancheran and Z. Huang, *Anal. Chem.*, 2009, **81**, 8908-8915, doi: 10.1021/ac9015159.
[48] H. Wu, J. V. Volponi, A. E. Oliver, A. N. Parikh, B. A. Simmons and S. Singh, *P. Natl. Acad. Sci. USA*, 2011, **108**, 3809-3814, doi: 10.1073/pnas.1009043108.
[49] F. Sun, T. Bai, L. Zhang, J.-R. Ella-Menye, S. Liu, A. K. Nowinski, S. Jiang and Q. Yu, *Anal. Chem.*, 2014, **86**, 2387-2394, doi: 10.1021/ac4040983.
[50] M. Lee, T.-I. Kim, K.-H. Kim, J.-H. Kim, M.-S. Choi, H.-J. Choi and K. Koh, *Anal. Biochem.*, 2002, **310**, 163-170, doi: 10.1016/s0003-2697(02)00384-6.
51. S. W. Bishnoi, C. J. Rozell, C. S. Levin, M. K. Gheith, B. R. Johnson, D. H. Johnson and N. J. Halas, *Nano Lett.*, 2006, **6**, 1687-1692, doi; 10.1021/nl060865w.
[52] N. Kanayama and H. Kitano, *Langmuir*, 2000, **16**, 577-583, doi: 10.1021/la990182e.
[53] A. Soni, R. K. Surana and S. K. Jha, *Senor. Actu. B: Chem.*, 2018, **269**, 346-353, doi : 10.1016/j.snb.2018.04.108.
[54] S. Morton, B. Crucian, S. Hagan, M. Satyamitra and A. Daily, In *NASA Technical Reports Server*; U.S. National Aeronautics and Space Administration: Washington, DC, USA, 2018.
[55] S. N. Thennadil, J. L. Rennert, B. J. Wenzel, K. H. Hazen, T. L. Ruchti and M. B. Block, *Diabetes Technol. The.*, 2001, **3**, 357-365, doi: 10.1089/15209150152607132.
[56] T. Reuveni, M. Motiei, Z. Romman, A. Popovtzer and R. Popovtzer, *Int. J. Nanomed.*, 2011, **6**, 2859, doi: 10.2147/IJN.S25446.
[57] J. Hainfeld, D. Slatkin, T. Focella and H. Smilowitz, *Brit. J. Radiol.*, 2006, **79**, 248-253, doi: 10.1259/bjr/13169882.
[58] D. C. Klonoff, D. Ahn and A. Drincic, *Diabetes Res. Clin. Pr.*, 2017, **133**, 178-192, doi: 10.1016/j.diabres.2017.08.005.
[59] D. DeSalvo and B. Buckingham, *Curr. Diab. Rep.*, 2013, **13**, 657-662, doi: 10.1007/s11892-013-0398-4.

Author information

Yikun Huang *is a PhD. Student in the Department of Biomedical Engineering, University of Connecticut, USA. She achieved her Bachelor degree in 2015 from Tianjin University, China. Her research focuses on SERS and bioluminescence based biosensing.*

